

Modeling Anthropomorphism in Dynamic Human Arm Movements

Pantelis T. Katsiaris, Panagiotis K. Artemiadis and Kostas J. Kyriakopoulos

Abstract— Human motor control has always acted as an inspiration in both robotic manipulator design and control. In this paper, a modeling approach of anthropomorphism in human arm movements during every-day life tasks is proposed. The approach is not limited to describing static postures of the human arm but is able to model posture transitions, in other words, dynamic arm movements. The method is based on a novel structure of a Dynamic Bayesian Network (DBN) that is constructed using motion capture data. The structure and parameters of the model are learnt from the motion capture data used for training. Once trained, the proposed model can generate new anthropomorphic arm motions. These motions are then used for controlling an anthropomorphic robot arm, while a measure of anthropomorphism is defined and utilized for assessing resulted motion profiles.

I. INTRODUCTION

Although arm motor control research has been going on for almost three decades [1], [2], there is still no clear mathematical parameterization, describing the vast repertoire of arm motions. However, human motor control has always acted as an inspiration for robotic systems design [3] and control [4], [5]. Robot arms resembling human arms in terms of kinematic dexterity and dynamically smooth behavior, can prove very useful in many complex industrial (i.e. welding, assembly etc.) and non-industrial tasks (i.e. rehabilitation, human motion assistance, entertainment robots etc.). Therefore, modeling anthropomorphism in a large repertoire of arm motions is very critical for both understanding human motor control principles, and designing control architectures for advanced robot arms.

For planar human arm motion, it has been confirmed that the human arm tends to follow a straight line, with bell-shaped tangential velocity profile [2]. Similar models, in terms of kinematics, were proposed later [6], while more complex models in terms of musculo-skeletal control have also been proposed [7], [8], [9]. However most of the previous research on arm movement has focused on planar motions, which limits the applicability of the proposed models, which can not be used to describe multi-joint arm movements required for even simple every-day tasks.

During the last decade, more sophisticated motion capture systems became available, and thus multi-joint coordination was analyzed. Specifically in the fields of robotics and computer animation, motion capture systems are nowadays

P. K. Artemiadis is with the Department of Mechanical Engineering, Massachusetts Institute of Technology (MIT), Cambridge, MA, USA. Email: partem@mit.edu.

P. T. Katsiaris and K. J. Kyriakopoulos are with the Control Systems Lab, School of Mechanical Eng., National Technical University of Athens, 9 Heron Polytechniou Str, Athens, 157 80, Greece. Email: pkatsiar@mail.ntua.gr, kkyria@mail.ntua.gr.

used in order to track human movements and build human motion databases. Then, the motion data are processed to find posture similarities [10] or define optimal paths for certain hand positioning [11]. A large number of methodologies have been proposed for modeling arm movements, such as Hidden Markov Models (HMMs) and Factorial HMMs [12], [13]. The definition of motor primitives (i.e. bases that can form multi-joint arm configurations) was recently introduced primarily for robot applications [14], while binary trees were also used for modeling human motion data [15]. Inter-joint dependencies in static human arm postures were modeled by the authors in [16]. However, most of the previous methods proposed could not capture the dynamic features of arm motions, because they were based on human motion data conceived as a set of discrete postures. Since modeling anthropomorphism in human arm movements strongly depends on the motion dynamic features, a model that can capture discrete postures transitions is required.

In this paper, a novel form of a Dynamic Bayesian Network (DBN) is proposed for the modeling of three-dimensional (3D) human arm motion, which is able to capture both discrete arm postures and posture transitions. Human motion capture data are collected during every-day-life arm tasks (i.e. reaching and grasping objects in the 3D space, moving the hand along surfaces etc). Discrete arm postures, extracted from the motion capture data set, are first modeled in joint space using a directed graphical model. Then a dynamic bayesian network is constructed, taking into account the directed graphical model, in order to describe discrete posture transition, i.e. dynamic arm motion. The proposed model can be used to generate new¹ anthropomorphic arm motions. The generated motion profiles are used to control an anthropomorphic robot arm, while tested for anthropomorphism using an appropriately defined criterion.

The rest of the paper is organized as follows: the proposed methodology is presented in Section II. The experimental procedure assessing the method efficiency is reported in Section III, while Section IV concludes the paper.

II. MODELING AND GENERATING ANTHROPOMORPHIC MOTION

A. Human Arm Motion Data Set

The human upper limb is a quite complex structure, composed of three chained *modules*, the shoulder girdle, the elbow and the wrist. Each *module* can be modeled as consisting

¹Continuous profiles that are not identical to those recorded in the motion capture data are considered as new motions.

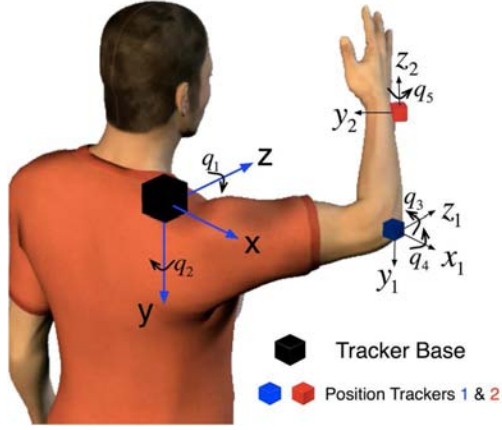


Fig. 1. The two position trackers are placed on the user's elbow and wrist joint, while the tracker reference system is placed on the user's shoulder. Rotation axes and positive directions for the 5 modeled degrees of freedom are shown.

of revolute joints since their translations are negligible compared to rotations. Therefore the human arm can be modeled as a 7 degrees of freedom (DoFs) mechanism, where 3 DoFs are located at the shoulder, 2 at the elbow and 2 at the wrist. In our approach we focus only on the first five DoFs, since, for simplicity reasons, the wrist is excluded. The 5 DoFs that will be analyzed are: shoulder abduction-adduction, shoulder flexion-extension, shoulder external-internal rotation, elbow flexion-extension and elbow pronation-supination. Let q_1, q_2, q_3, q_4, q_5 be the five corresponding joint angles of those DoFs.

A motion capture system (Isotrak II, Polhemus Inc.) is used for recording human arm motion. It is equipped with a reference system, with respect to which, the 3D position and orientation of two position tracking sensors is provided. The frequency of the measurements is 30 Hz. The reference system is placed on the shoulder, while one sensor is placed on the elbow and the second one on the wrist. The sensors placement along with the defined joint angles is shown in Fig. 1.

Let $\mathbf{T}_1 = [x_1 \ y_1 \ z_1]^T$, $\mathbf{T}_2 = [x_2 \ y_2 \ z_2]^T$ denote the position of the trackers with respect to the tracker reference system. By solving the inverse kinematic equations the human joint angles are given by:

$$\begin{aligned}
 q_1 &= \arctan 2 (\pm y_1, x_1) \\
 q_2 &= \arctan 2 \left(\pm \sqrt{x_1^2 + y_1^2}, z_1 \right) \\
 q_3 &= \arctan 2 (\pm B_3, B_1) \\
 q_4 &= \arctan 2 \left(\pm \sqrt{B_1^2 + B_3^2}, B_2 - L_1 \right) \\
 q_5 &= \arctan 2 (M, \Lambda) + \arctan 2 \left(1 \pm \sqrt{\frac{K^2}{M^2 + \Lambda^2}}, \frac{K}{\sqrt{M^2 + \Lambda^2}} \right)
 \end{aligned} \tag{1}$$

where

$$\begin{aligned}
 B_1 &= x_2 \cos(q_1) \cos(q_2) + y_2 \sin(q_1) \cos(q_2) - z_2 \sin(q_2) \\
 B_2 &= -x_2 \cos(q_1) \sin(q_2) - y_2 \sin(q_1) \sin(q_2) - z_2 \cos(q_2) \\
 B_3 &= -x_2 \sin(q_1) + y_2 \cos(q_1) \\
 K &= \tan(\phi) (\cos(q_2) \cos(q_4) - \cos(q_3) \sin(q_2) \sin(q_4)) \\
 \Lambda &= \sin(q_2) \sin(q_3) \\
 M &= \cos(q_3) \cos(q_4) \sin(q_2) + \cos(q_2) \sin(q_4)
 \end{aligned} \tag{2}$$

where ϕ the roll angle measured from the position tracker 2 and L_1 the length of the upper arm. The length of the upper arm can be computed from the distance of the first position tracker from the base reference system, i.e. $L_1 = \|\mathbf{T}_1\| = \sqrt{x_1^2 + y_1^2 + z_1^2}$. Likewise, the length of the forearm L_2 can be computed from the distance between the two position trackers, i.e. $L_2 = \sqrt{(x_2 - x_1)^2 + (y_2 - y_1)^2 + (z_2 - z_1)^2}$. Finally, one of the multiple solutions of (1) is selected at each time instance, based on the corresponding human joint motion ranges and the previous solution selection. For the complete analysis of the inverse kinematics the reader should refer to [17].

Using the motion capture system, arm motion during every-day life tasks² was measured. Then, using the inverse kinematics presented above, a data set of P arm postures each one consisting of 5 joint angles (q_1, \dots, q_5) is available. For the subsequent analysis $P = 10000$ arm postures were used, which corresponds to approximately 5.5 minutes of motion recording.

B. Modeling Static Arm Postures

Modeling of human arm movement has received increased attention during the last decades, especially in the field of robotics [18] and graphics. This is because there is a great interest in modeling and understanding underlying laws and motion dependencies among the DoFs of the arm, in order to incorporate them into robot control schemes. Most of the previous works in this area focus on the definition of motor primitives [19], or on objective functions that are minimized during arm motion. These models lack the ability to describe dependencies among the DoFs of the arm though. In this paper, in order to model the dependencies among the DoFs of the arm during random 3D movements, graphical models are used.

1) *Graphical Models*: Graphical models are a combination of probability theory and graph theory. They provide a tool for dealing with two characteristics; the uncertainty and the complexity of random variables. Given a set $\mathbf{F} = \{f_1 \dots f_N\}$ of P random variables with joint probability distribution $p(f_1, \dots, f_N)$, a graphical model attempts to capture the conditional dependency structure inherent in this distribution, essentially by expressing how the distribution factors as a product of *local functions*, (e.g. conditional probabilities) involving various subsets of \mathbf{F} . Directed graphical models, is a category of graphical models,

²Tasks performed during training involve reach and grasp objects located in different positions in the arm workspace, wiping a horizontal and vertical flat surface etc.

also known as Bayesian Networks. A directed acyclic graph is a graphical model where there are no graph cycles when the edge directions are followed. Given a directed graph $G = (V, E)$, where V is the set of vertices (or nodes) representing the variables f_1, \dots, f_N , and E is the set of directed edges between those vertices, the joint probability distribution can be written as follows:

$$p(f_1, \dots, f_N) = \prod_{i=1}^N p(f_i | a(f_i)) \quad (3)$$

where, $a(f_i)$ the *parents* (or direct ancestors) of node f_i . If $a(f_i) = \emptyset$ (i.e. f_i has no parents), then $p(f_i | \emptyset) = p(f_i)$, and the node i is called the *root* node.

2) *Building the Model*: A version of a directed graphical model is a tree model. It's restriction is that each node has only one parent. The optimal tree for a set of variables is given by the Chow-Liu algorithm [20]. Briefly, the algorithm constructs the maximum spanning tree of the complete mutual information graph, in which the vertices correspond to the variables of the model and the weight of each directed edge $f_i \rightarrow f_j$ is equal to the mutual information $I(f_i, f_j)$, given by

$$I(f_i, f_j) = \sum_{f_i, f_j} p(f_i, f_j) \log \frac{p(f_i, f_j)}{p(f_i)p(f_j)} \quad (4)$$

where $p(f_i, f_j)$ the joint probability distribution function for f_i, f_j , and $p(f_i), p(f_j)$ the marginal distribution probability functions for f_i, f_j respectively. Mutual information is a unit that measures the mutual dependence of two variables. The most common unit of measurement of mutual information is the bit, when logarithms to the base of 2 are used. It must be noted that the variables $\{f_1 \dots f_N\}$ are considered discrete in the definition of (4). Details about the algorithm of the maximum spanning tree construction can be found in [20].

In our case, the variables $\{q_1, q_2, q_3, q_4, q_5\}$ correspond to the joint angles of the 5 modeled DoFs of the arm. If these are rounded to the nearest integer, then, with a maximum rounding error of 0.5 deg, joint variables are essentially discretized, enabling the simplification of the directed graphical model training and inference algorithms, without essential loss of information due to discretization. Using joint angle data recorded during the training phase, we can build the tree model. The resulting tree structure is shown in Fig. 2. This graphical model essentially describes the inter-joint dependencies of human arm static postures. In order to construct a model that will describe dynamic arm motions, a Dynamic Bayesian Network will be constructed, in order to model the dynamic behavior of the nodes consisting this static directed graphical model.

C. Modeling Dynamic Arm Motions

In order to model the dynamic behavior of the nodes appearing in the static model, we define a dynamic bayesian network that essentially consists of two instances of the static model, connected to each other through the corresponding

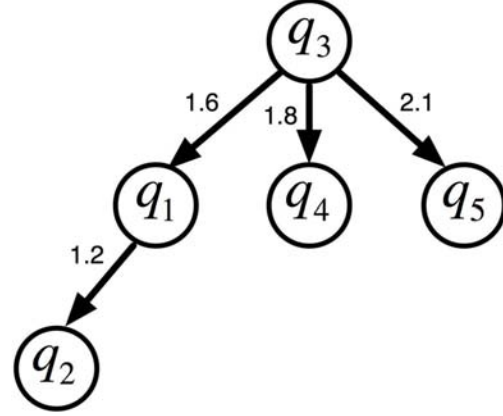


Fig. 2. The directed graphical model (tree) representing nodes (i.e. joint angles) dependencies. Representation $q_i \rightarrow q_j$ means that node q_i is the parent of node q_j , where $i, j = 1, 2, 3, 4, 5$. The mutual information $I(q_i, q_j)$ is shown at each directed edge connecting q_i to q_j . The value of the mutual information quantifies the information gained if we describe two variables through their dependency, instead of considering them as independent. Its value is in bits.

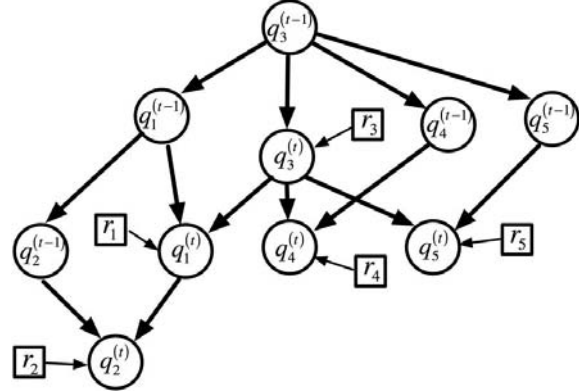


Fig. 3. The dynamic Bayesian Network graph describing the relationship among the five joint angles of the human arm q_i^t at time t and their previous values q_i^{t-1} , $i = 1, 2, 3, 4, 5$. Thick arrows describe dependence, while thin arrows, connecting the independent random variables r_i with the joint angles q_i^t , correspond to algebraic addition.

nodes. Using this formulation, the dynamic behavior of the nodes is introduced in the model, while the inter-joint dependencies are modeled through the underlying static graphs. Moreover, a random variable is also added in the dynamics of each node, for purposes analyzed below. The complete dynamic bayesian network is shown in Fig. 3. As it can be seen, each joint angle q_i , $i = 1, 2, 3, 4, 5$, at time t , can be dependent either to only its previous value $q_i(t-1)$ or to its previous value and to the current value of another angle.

Moreover, to each joint angle value, a random variable r_i , $i = 1, 2, 3, 4, 5$, is added. This is done to avoid stalling into a narrow region of joint angles for each joint and to allow a normal joint angle variation within a time instance (i.e. angular velocity). Therefore, adding a random variable at the evolution of the joint angles permits the angle to

vary considerably between successive steps. However, this should happen between the observed range during training. Therefore, each random variable r_i is drawn from a zero-mean Gaussian distribution $\mathcal{N}(0, \sigma_i)$, where the variance σ_i for each joint angle is computed using the variance of the angular velocities observed from the training data.

Having the full form of the dynamic graphical model, the overall joint probability distribution of the model can be computed. It must be noted that for each time instance t , the values of all the joint angles at the previous time instance $t - 1$ are considered known. Therefore, the values of each joint angle at time t are drawn by the following conditional probability:

$$p\left(q_1^{(t)}, q_2^{(t)}, q_3^{(t)}, q_4^{(t)}, q_5^{(t)} \mid q_1^{(t-1)}, q_2^{(t-1)}, q_3^{(t-1)}, q_4^{(t-1)}, q_5^{(t-1)}\right) = p_1 p_2 p_3 p_4 p_5 \quad (5)$$

where

$$\begin{aligned} p_1 &= p\left(q_1^{(t)} \mid q_1^{(t-1)}, q_3^{(t)}\right) + p(r_1) \\ p_2 &= p\left(q_2^{(t)} \mid q_2^{(t-1)}, q_1^{(t)}\right) + p(r_2) \\ p_3 &= p\left(q_3^{(t)} \mid q_3^{(t-1)}\right) + p(r_3) \\ p_4 &= p\left(q_4^{(t)} \mid q_4^{(t-1)}, q_3^{(t)}\right) + p(r_4) \\ p_5 &= p\left(q_5^{(t)} \mid q_5^{(t-1)}, q_4^{(t)}\right) + p(r_5) \end{aligned} \quad (6)$$

where $q_i^{(t)}$, $q_i^{(t-1)}$ denote the values of joint angle q_i at time instances t and $t-1$ respectively and $p(r_i)$ are the probability distributions of the random variables r_i , $i = 1, 2, 3, 4, 5$, given by:

$$p(r_i) = \frac{1}{\sigma_i \sqrt{2\pi}} e^{-\frac{r_i^2}{2\sigma_i^2}} \quad (7)$$

From (6) it is obvious that there are some joint angles that are dependent only on their previous values (i.e. q_3), while others that depend on the current values of others too (i.e. q_1, q_2, q_4, q_5). The dependencies of the current joint angles to both the past and the other current joint angles are described by the conditional probability distributions in (6). However, these functions are based on finite measurements of joint angles during the human arm motion experiments. More specifically, a 2-dimensional histogram can be constructed for probability distributions involving two variables (i.e. $p\left(q_3^{(t)} \mid q_3^{(t-1)}\right)$). Accordingly, a 3-dimensional histogram can be constructed for the other angles that are dependent both on their history and the other angles. A way to conclude to a continuous representation of those discrete histograms, is to fit to them continuous functions of probability density. These functions are selected to be Gaussian Mixture Models (GMMs) [21]. A GMM is essentially a weighted sum of Gaussian distribution functions, that can describe quite efficiently complex and non-smooth probability distribution functions. In general, for a n -dimensional GMM, the probability distribution function is given by:

$$p(\mathbf{Q}) = \sum_{k=1}^h \pi_k \mathcal{N}(\mathbf{M}_k, \mathbf{S}_k) \quad (8)$$

where h is the number of mixture components and $\mathcal{N}(\mathbf{M}_k, \mathbf{S}_k)$ is a n -dimensional Gaussian distribution function with mean matrix \mathbf{M}_k and covariance matrix \mathbf{S}_k respectively. Details about the GMMs and their fitting procedure (Expectation Maximization (EM)) can be found in [21].

Fitting each one of the conditional probability functions in (6) with a Gaussian Mixture Model, concludes to a continuous representation of the probabilities involved in estimating each joint angle, which essentially serves two main scopes; firstly, it smoothes the conditional histograms created using the recorded data, and secondly, it allows for a more computational effective way of producing values for the joint angles that is now based on continuous mathematical formulas instead of discrete and high-dimensionable search-

able tables.

D. Generating Anthropomorphic Motions

Generation of anthropomorphic arm motions using the previously defined model is based on performing statistical inference for the unknown nodes of the model. In our case, we can decide an initial configuration of the arm, and calculate the next values for all the joint angles, using the fitted GMM distributions for the conditional probability functions that govern the model (see (6)). The initial values should be drawn within the range of recorded motion for each joint angle, however this is not a hard constraint, since the model can easily converge to human-like configurations based on the inherently described anthropomorphic kinematics.

Therefore, if the initial configuration of the arm is decided to be $\mathbf{q}_0 = \left[q_1^{(t-1)} \quad q_2^{(t-1)} \quad q_3^{(t-1)} \quad q_4^{(t-1)} \quad q_5^{(t-1)} \right]^T$, then *sequentially*, using the GMM distributions functions fitted to the conditional probability functions p_3, p_1, p_2, p_4 and p_5 , the next joint angles $\mathbf{q}_t = \left[q_1^{(t)} \quad q_2^{(t)} \quad q_3^{(t)} \quad q_4^{(t)} \quad q_5^{(t)} \right]^T$ can be computed. It must be noted that the independent random variables r_i , $i = 1, 2, 3, 4, 5$ are added at each joint angle after the GMM function computation, since they are considered independent of the joint angles and their history.

III. RESULTS

A. Generated vs Human Arm Movements

Using the model proposed in this work and the method analyzed in Section II.D, a continuous anthropomorphic arm motion is generated in joint space. Let $\mathbf{q}_G = \left[\mathbf{q}_{G1} \quad \mathbf{q}_{G2} \quad \mathbf{q}_{G3} \quad \mathbf{q}_{G4} \quad \mathbf{q}_{G5} \right]$ be a $\eta \times 5$ matrix including the η -point trajectory of each joint i , where \mathbf{q}_{Gi} is a κ -dimensional vector of the trajectory of joint i , $i = 1, 2, 3, 4, 5$, $\eta, \kappa \in \mathbb{R}$. In order to compare this model-generated motion with the corresponding executed by a human, and to assess its anthropomorphic characteristics, a human should perform the same task. For this reason, a 7 DoF anthropomorphic manipulator (PA-10, Mitsubishi Heavy Industries) is used in an appropriately designed setup analyzed below. Details on the modeling of the robot arm can be found in [22].

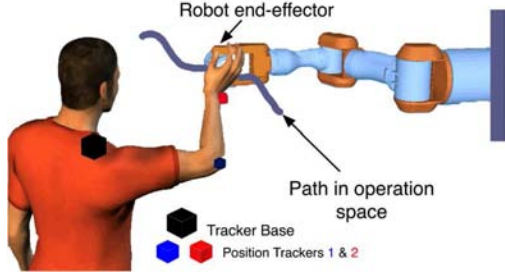


Fig. 4. The experimental protocol used for moving the human arm along a predefined path in the arm operational space. The position tracking system is used for monitoring human arm motion in the joint space. The human hand is attached to the robot end-effector at the wrist, so the subject should move only the elbow and the shoulder for following the robot motion.

In order to make the human perform the same motion in the operational space, the setup depicted in Fig. 4 is used. The human is standing opposite to a robot arm while his/her hand is firmly attached to the robot end-effector, at a point just before the wrist. Therefore, the human is able to follow the robot trajectory in the 3D space, appropriately configuring only the elbow and shoulder joints. The position tracking sensors used during the model training are used again on the human's arm in order to record the performed motion. Using these measurements, the human arm trajectory in the joint space is then computed. Regarding the path imposed by the robot arm, it is computed through the generated motion profiles in joint space, after being reformed to the robot operational space using forward kinematics of a model of the human arm. In other words, having the generated motion in joint space, the human arm trajectory in the 3D space is computed through human arm forward kinematics. Then, in order for the robot arm to move its end-effector (and consequently the human hand) along this path, the trajectory is first transformed to the robot base reference system, and then through robot inverse kinematics, the path in the robot joint space is computed. An inverse dynamic controller is finally used at the robot arm to track the desired trajectory.

In Fig. 5 the generated and the human arm trajectories in joint space for each joint are shown. It appears that the two profiles of motion are very similar, not only in the kinematic but also in the dynamic level, essentially confirming the anthropomorphic characteristics of the model-generated motion.

B. Quantifying Anthropomorphism

The anthropomorphism in the generated motion can be also proved by the statistical resemblance between the robot and the human arm motion. One of the criteria that were used in the past to identify and quantify inherent relationships between two or more variables is the Mutual Information (MI) index [23]. The mutual information definition between two sets of variables was given in Section II in (4). However, in this case, since we want to discuss the joint probability distribution of the two sets (i.e. the generated and the human

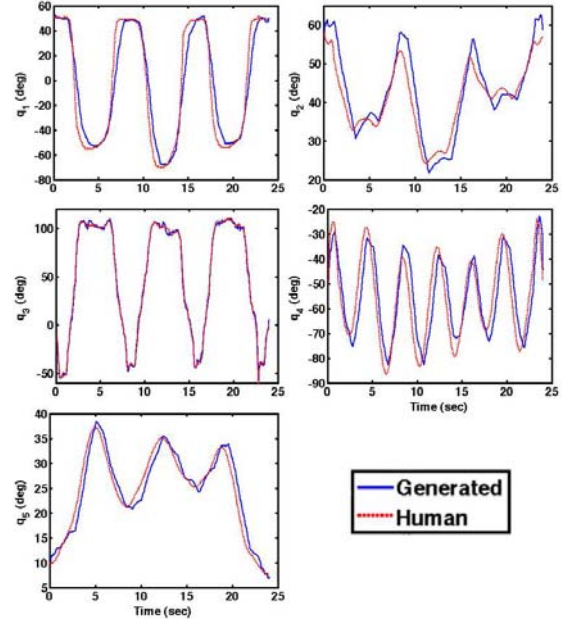


Fig. 5. Generated versus human performed motion in the joint space for the same path in the operation 3D space.

TABLE I
INDIVIDUAL AND JOINT ENTROPIES OF THE MODEL-GENERATED AND THE HUMAN ARM MOTION SETS ALONG WITH RESULTED VALUES OF THE MUTUAL INFORMATION (MI) INDEX.

i	$H(q_{G_i})$	$H(q_{H_i})$	$H(q_{G_i}, q_{H_i})$	$I(q_{G_i}, q_{H_i})$
1	5.44	5.38	7.26	3.56
2	4.91	5.04	7.43	2.51
3	6.19	6.19	6.19	6.19
4	5.96	6.03	7.99	4.00
5	4.95	4.96	7.27	2.64

motion), the MI will be defined in a form including the individual and joint entropies of the two sets. Therefore, it is equivalently defined by:

$$I(q_{G_i}, q_{H_i}) = H(q_{G_i}) + H(q_{H_i}) - H(q_{G_i}, q_{H_i}) \quad (9)$$

where q_{G_i} , q_{H_i} represent the set of values for the model-generated and the human joint angles observed during the previously analyzed experiment, where $i = 1, 2, 3, 4, 5$ corresponds to the 5 joint angles, while $H(q_{G_i})$, $H(q_{H_i})$ are the Shannon entropies of the two sets and $H(q_{G_i}, q_{H_i})$ is the joint entropy of the two sets. The individual and joint entropies along with the resulted MI values for the model-generated and the human angle sets, are reported in Table I. From the values computed, it appears that the generated motion has strong inherent resemblance with the motion the human arm performed, therefore can be considered anthropomorphic.

IV. DISCUSSION AND CONCLUSIONS

The human arm mechanics, its dexterity, and its vast repertoire of motion still remain a great inspiration for

robot design and control. For this reason, a mathematical formulation of the inherent characteristics that the motion of the human arm possesses, is of great interest, since it can be used for controlling robots in performing tasks in an anthropomorphic way. Most of the previous studies in this field could capture and mimic static human arm postures, but were unable to generate new motions that would be anthropomorphic too. In this paper, we propose a method modeling anthropomorphism in human arm motions, in such way, that it can generate new motion patterns that would obey to anthropomorphic characteristics. The method is based on the fact that not only static arm postures are modeled, but also the transitions between those postures, i.e. the dynamic effects of the human arm motion. A dynamic Bayesian network was used, that proved able to encapsulate human motion characteristics. The method was tested in generating anthropomorphic motion for controlling a robot arm, while a measure of anthropomorphism in arm motion was introduced and utilized for assessing the resulted motion. The results showed that the method can be used for generating anthropomorphic motions that can be eventually used for controlling robots.

Other methods for capturing dynamic characteristics of arm motion could have been used, e.g. Factorial HMMs [12], [13]. However these models abstract the modeled data as stochastic representations. In the contrary, the DBN used in this work, is not a stochastic representation but it represents each variable of the physical system with a distinct node. Unlike with HMMs, the proposed model was not used for extracting patterns of motion that are combined in order to reconstruct or generate new movements. It was efficiently used to model inter-joint dependencies in an analytic way and generate new arm motions based on the anthropomorphic characteristics “embodied” in the model through training.

It must be noted that the method was tested for voluntary and unconstrained arm motions. Therefore the interaction of the arm with the environment, by exerting forces to objects or lifting objects, is not included in the study. This would require the study of the adaptations taking place in kinematic level for adjusting to planned or unforeseen change of the arm dynamics. However, this is out of the scope of this paper, where only unconstrained motions are being studied. In terms of using this methodology for controlling robot arm though, the interaction with the environment and the change in dynamics could be easily accommodated by using the appropriate control schemes, while having as reference trajectories the ones generated by the proposed method.

ACKNOWLEDGMENT

This work has been partially supported by the European Commission with the Integrated Project no. 248587, “THE Hand Embodied”, within the FP7-ICT-2009-4-2-1 program “Cognitive Systems and Robotics”.

REFERENCES

[1] P. Morasso, “Spatial control of arm movements,” *Exp. Brain Res.*, vol. 42, pp. 223–227, 1981.

[2] T. Flash and N. Hogan, “The coordination of arm movements: an experimentally confirmed mathematical model,” *J Neurosci*, vol. 5, pp. 1688–1703, 1985.

[3] K. Berns, T. Asfour, and R. Dillmann, “Design and control architecture of an anthropomorphic robot arm,” *International Conference on Advanced Mechatronics*, 1998.

[4] V. Potkonjak, M. Popovic, M. Lazarevic, and J. Sinanovic, “Redundancy problem in writing: From human to anthropomorphic robot arm,” *IEEE Transaction on Systems, Man and Cybernetics, part B*, vol. 28, pp. 790–805, 1998.

[5] V. Caggiano, A. D. Santis, B. Siciliano, and A. Chianese, “A biomimetic approach to mobility distribution for a human-like redundant arm,” *Proc. of the IEEE/RAS-EMBS International Conference on Biomedical Robotics and Biomechanics*, pp. 393–398, 2006.

[6] B. Hoff and M. Arbib, “Models of trajectory formation and temporal interaction of reach and grasp,” *Journal of Motor Behavior*, vol. 25, pp. 175–192, 1993.

[7] H. Gomi and M. Kawato, “The change of human arm mechanical impedance during movements under different environmental conditions,” *Society for Neuroscience Abstracts*, vol. 21:686, 1996.

[8] Y. Uno, M. Kawato, and R. Suzuki, “Formation and control of optimal trajectory in human multijoint arm movement,” *Biological Cybernetics*, vol. 61, pp. 89–101, 1989.

[9] H. Tanaka, M. Tai, and N. Qian, “Different predictions by the minimum variance and minimum torque-change models on the skewness of movement velocity profiles,” *Neural Computation*, vol. 16:10, pp. 2021–2040, 2004.

[10] L. Kovar, M. Gleicher, and F. Pighin, “Motion graphs,” *ACM Transactions on Graphics*, vol. 21:3, pp. 473–482, 2002.

[11] J. Lee, J. Chai, P. Reitsma, J. Hodgins, and N. Pollard, “Interactive control of avatars animated with human motion data,” *ACM Transactions on Graphics*, vol. 21:3, pp. 491–500, 2002.

[12] T. Inamura, I. Toshima, H. Tanie, and Y. Nakamura, “Embodied symbol emergence based on mimesis theory,” *The International Journal of Robotics Research*, vol. 23:3-5, pp. 363–377, 2004.

[13] D. Kulic, W. Takano, and Y. Nakamura, “Representability of human motions by factorial hidden markov models,” *Proc. of IEEE/RSJ Int. Conf. Intelligent Robots and Systems*, pp. 2388–2393, 2007.

[14] —, “Incremental learning, clustering and hierarchy formation of whole body motion patterns using adaptive hidden markov chains,” *The International Journal of Robotics Research*, vol. 27:7, pp. 761–784, 2008.

[15] K. Yamane, Y. Yamaguchi, and Y. Nakamura, “Human motion database with a binary tree and node transition graphs,” *Robotics: Science and systems V*, 2009.

[16] P. K. Artemiadis, P. T. Katsiaris, and K. J. Kyriakopoulos, “A biomimetic approach to inverse kinematics for a redundant robot arm,” *Autonomous Robots*, (in press), 2010.

[17] P. K. Artemiadis and K. J. Kyriakopoulos, “A bio-inspired filtering framework for the EMG-based control of robots,” in *Proc. of 17th Mediterranean Conference on Control and Automation*, 2009.

[18] A. Billard and M. J. Mataric, “Learning human arm movements by imitation: Evaluation of a biologically inspired connectionist architecture,” *Robotics and Autonomous Systems*, vol. 37:2-3, pp. 145–160, 2001.

[19] A. Fod, M. J. Mataric, and O. C. Jenkins, “Automated derivation of primitives for movement classification,” *Autonomous Robots*, vol. 12(1), pp. 39–54, 2002.

[20] C. K. Chow and C. N. Liu, “Approximating discrete probability distributions with dependence trees,” *IEEE Transactions on Information Theory*, vol. 14(3), pp. 462–467, 1968.

[21] G. McLachlan and D. Peel, *Finite mixture models*. John Wiley & Sons, Inc, 2000.

[22] N. A. Mpompos, P. K. Artemiadis, A. S. Oikonomopoulos, and K. J. Kyriakopoulos, “Modeling, full identification and control of the mitsubishi PA-10 robot arm,” *Proc. of IEEE/ASME International Conference on Advanced Intelligent Mechatronics, Switzerland*, 2007.

[23] R. Steuer, C. O. Daub, J. Selbig, and J. Kurths, *Measuring Distances Between Variables by Mutual Information*. Springer Berlin Heidelberg, 2005.